Distributed Secondary Control and Management of Islanded Microgrids via Dynamic Weights

Li, Qiang; Peng, Congbo; Wang, Minglin; Chen, Minyou; Guerrero, Josep M.; Abbott, Derek

Published in:
IEEE Transactions on Smart Grid

DOI (link to publication from Publisher):
10.1109/TSG.2018.2791398

Publication date:
2019

Document Version
Accepted author manuscript, peer reviewed version

Distributed Secondary Control and Management of Islanded Microgrids via Dynamic Weights

Qiang Li, Congbo Peng, Minglin Wang, Minyou Chen, *Senior Member, IEEE,* Josep M. Guerrero, *Fellow, IEEE* and Derek Abbott, *Fellow, IEEE*

***Abstract*—The averaging algorithm for consensus is widely used as a distributed secondary method for the control and management of microgrids. However, during each iteration it may break the system balance obtained by the primary control. In this paper, a distributed and networked method for the control and management of islanded microgrids is proposed, in which there is an agent based communication network as the top layer over a microgrid as the bottom layer. Further, a systematic method is presented to derive a set of distributed control laws for agents from any given communication network, where only nearest neighbor information is needed. The control laws consist of two terms, dynamic and fixed weights, in which the term with dynamic weights reassigns outputs of distributed generators in order to reach different targets. Moreover, this method offers a convenient way to achieve different targets of control and management by substituting a parameter in the control laws with dynamic weights. More importantly, the control laws with dynamic weights never break the system balance during iterations. We formally show that if agents apply the control laws to regulate distributed generators, their outputs will iteratively satisfy the given targets. Finally, simulations are carried out to evaluate the performance of the control laws. The results show that equal outputs, proportional outputs and the optimal incremental cost are obtained. Moreover, the voltage and frequency are still stable, when fluctuations of load demand and environmental conditions are considered.**

***Index Terms*—Distributed control, energy management, microgrids, multi-agent system (MAS), networked control systems, secondary control.**

I. Introduction

NOWADAYS, most environmental problems are strongly associated with the combustion of nonrenewable fossil fuels. Therefore, more countries are progressively switching to the utilization of renewable energy, which appears to be an ideal solution for reducing pollution [1]. Renewable power generation is emerging as a flexible way to penetrate the grid, replacing traditional energy sources [2]. Presently, distributed generators (DGs) using renewable energies and other equipment are generally integrated as a microgrid (MG), which can run independently (islanded mode) or be connected to a main grid (grid-connected mode) so as to reduce the perturbation on the grid [3], [4]. It is considered more complex to control an islanded MG, because of its low equivalent inertia and the uncertainty of DG outputs and fluctuations of load demand.

During the last decade, much interest has been focused on the control of MGs, where the control schemes mainly have three types, i.e., hierarchical control [5]–[8], centralized control [9]–[12], and decentralized or distributed control [13]–[16]. Hierarchical control consists of primary control, secondary control, and sometimes tertiary control, where DGs are regulated by the primary control, while the deviation introduced by primary control is eliminated by the secondary control. In centralized control, there is an MG central controller (MGCC) that collects and processes all information, so optimal solutions can be obtained without iterations. However, a failure in the MGCC will result in a total system break down. On the other hand, in decentralized or distributed control, only local information is used, and the system can still work even if several agents fail, but optimal solutions will be reached by iterations. To reduce the complexity of communication and computation, decentralized or distributed control seems more plausible, which has three main branches, namely, consensus based algorithms, multi-agent system (MAS) based methods and their combination.

Note that MAS methods have been widely applied in distributed control of MGs because of their distributed nature. When several MGs were integrated as a large system, an MAS-based hierarchical control method was presented [17] and then it was extended to a four-level hierarchical method in order to improve the comprehensive performance of the large system, where agents at different levels share responsibilities and also interact in a cooperative manner [18]. In a droop controlled islanded MG, errors in active power sharing may be produced by self-frequency recovery control employing distributed control, so a compensation control method was developed to eliminate the errors and share active power more accurately [19]. Meanwhile, MAS is also applied to achieve economic dispatch in MGs [20], [21].

In recent years, consensus algorithms or consensus protocol as the paradigm of distributed methods have attracted much attention. Schiffer et al. [22] proposed a consensus-based distributed voltage control method for meshed inverter-based MGs and provided a rigorous mathematical analysis to the existence and uniqueness of an equilibrium point of the voltage and reactive power dynamics. To share currents among DGs more accurately and ensure voltage unbalance compensation, a distributed negative sequence current sharing method based on a dynamic consensus algorithm was given [23]. Further,

Q. Li, C. Peng and M. Chen are with the State Key Laboratory of Power Transmission Equipment & System Security and New Technology, School of Electrical Engineering, Chongqing University, Chongqing 400044, China. (e-mail: qiangli.ac@gmail.com)

M. Wang is with Weifang power supply company, Weifang 261021, China.

J. M. Guerrero is with the Department of Energy Technology, Aalborg University, 9220 Aalborg East, Denmark.

D. Abbott is with the School of Electrical and Electronic Engineering, University of Adelaide, SA 5005, Australia.

Manuscript received XX, 2017; revised XX, 2017.

a consensus algorithm-based distributed hierarchical control method for DC MGs was presented, where a DC MG was modeled in the discrete time domain, and then a sensitivity analysis was performed when the interactive feature of the consensus algorithm and the MG was considered [24].

Furthermore, a multiagent-based consensus algorithm was developed to coordinate DGs in an Energy Internet [25], [26]. To restore the voltage and frequency of an MG in finite time, networked inverters were considered as a cooperative MAS, in which the consensus algorithm and feedback linearization approach were involved to ensure the convergence, and both frequency restoration and active power sharing were achieved by a finite-time control protocol, and the upper bounds on the convergence was given [27]. Moreover, consensus algorithms are extended to optimisation and management of MGs. Combining MAS with consensus algorithms, Xu et al. [28] proposed a fully distributed control strategy for the optimal management of resources, namely to maximize the overall welfare of all participants, in an islanded MG.

In summary, some methods are too complicated in the above mentioned papers, so that they cannot rapidly respond to system fluctuations. Moreover, although the averaging algorithm for consensus [29]–[31] is widely used as a distributed secondary method for the control and management of MGs, it may break the system balance during iterations. Furthermore, it does not provide unified steps in the design of algorithms for the control and management of MGs, which means one still has to design different algorithms to meet different requirements, such as proportional outputs and minimal costs. Therefore, a simple and unified method is needed, in which steps are given to derive a set of completely distributed control laws and to reach different requirements only requires the convenient substitution of a parameter in the control laws. More importantly, the control laws do not break the system balance during the iterations.

Moreover, in recent years, a number of innovative demonstration projects of islanded MGs have been built in China in order to test and measure the performance, where the active and reactive power control (PQ control) and voltage and frequency control (V/F control) modes are applied for primary control, while centralized control is applied for secondary control [32]–[34]. So far, these small islanded MGs work well for a long period of time. However, only a few studies have been performed in distributed control methods for PQ controlled MGs. Therefore, in this paper, a two layer distributed control method for PQ controlled MGs is presented, where the top layer is a communication network composed of agents, while the bottom layer is the MG.

In this paper, there are four main technical contributions. *First*, a simple and unified method is proposed, which offers unified steps to design algorithms for the control and management of MGs by changing a parameter in the control laws with dynamic weights. *Second*, a systematic method is presented, which gives the steps of how to derive a set of control laws with dynamic and fixed weights, where the control laws with dynamic weights reassign outputs of DGs in order to reach different targets iteratively. *Third*, during iterations, the control laws with dynamic weights do not disturb the system, which means the control laws never break the supply-demand balance, even if outputs are reassigned among controllable DGs. *Fourth*, theorems and a proposition are proved, which guarantee the outputs of DGs will satisfy given requirements iteratively, if agents regulate DGs in terms of the control laws.

The rest of the paper is organized as follows. In Section II, the topology of the communication network is given first, and then the steps of how to derive the control laws are presented. Later, the convergence properties of the control laws are analyzed. Section III introduces the structure of the MG and the parameters of DGs for simulations. In Section IV, eight cases are designed to evaluate the performance of the control laws, where some extreme situations are considered, and then simulation results are analyzed, discussed and compared. Section V concludes the paper.

II. Distributed Secondary Control and Management of MGs

In this section, some terms and the topology of a communication network are introduced first. And then, a systematic method is presented, which shows how the distributed control laws with dynamic weights for agents are derived from any given communication networks. Finally, theorems and a proposition are proved, which indicate the convergence of the control laws.

A. Topology of Communication Network

The distributed and networked method is a two-layer model, where the top layer is a communication network composed of agents, while the bottom layer is an MG composed of DGs, as shown in Fig. 1. Generally speaking, DGs, such as photovoltaic (PV) systems or wind turbines (WTs) are considered as *uncontrollable* or *non-dispatchable* DGs, for their outputs rely on environmental conditions. Conversely, DGs, such as microturbines (MTs) and fuel cells (FCs), are considered as *controllable* or *dispatchable* DGs because they can be regulated easily in terms of control signals. In an islanded MG, there is another type of DG, generally a battery energy storage system (BESS), called a *partially controllable* DG, which works in a V/F control mode, and provides the frequency and voltage references for the MG.

Correspondingly, the agents are called uncontrollable, controllable or partially controllable agents depending on the types of DGs to which they connect, as the links between two layers are shown in Fig. 1. Moreover, these agents form a communication network, which is a directed graph $G(V, E)$, where V is the set of agents (nodes), E is the set of edges (links). On this communication network, uncontrollable agents (indicated by circles) only have outgoing links that are represented by black arrow lines, because they do not deal with information but send information, such as the values of active and reactive power. In contrast, controllable agents (indicated by diamonds) may have outgoing and ingoing links that are represented by red arrow lines, which means they process information and at the same time transmit information to their neighbors. Also, they have self loops in order to collect their own information. The dashed arrow lines between two layers means information

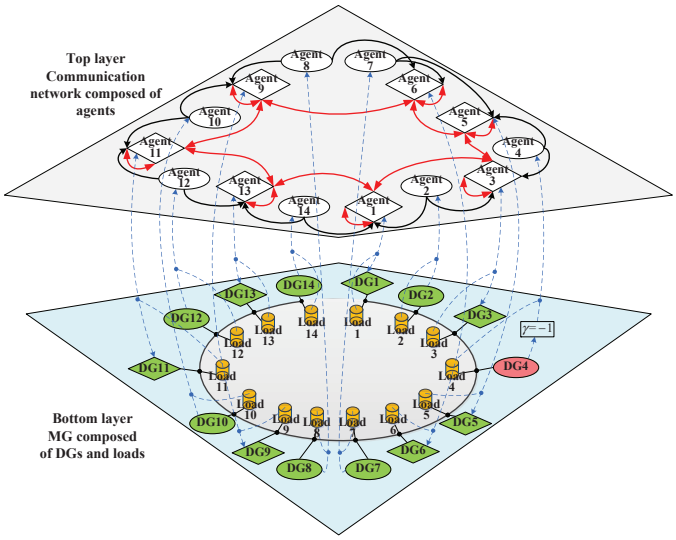

Fig. 1. The two-layer control model for MGs, where uncontrollable and partially controllable agents are indicated by circles, while controllable agents are indicated by diamonds.

can be collected from DGs and loads, and also can be sent to controllable DGs.

Additionally, for an islanded MG, a BESS working in a V/F control mode is generally needed, which provides the frequency and voltage references for the MG. As is known, the BESS will inject or absorb power into or from the MG in order to balance the system, if there are fluctuations in the MG. However, if the injection or absorption lasts for a long time, it will be possible that the state of charge of the BESS is lower than the minimal level or reaches saturation, which is not conducive to dealing with fluctuations. Therefore, the outputs of the BESS are considered as loads by adding the parameter $\gamma = -1$ between DG_4 (the BESS or the V/F DG) and its agent. Thus, the V/F DG provides the system losses instantaneously, and then its outputs are shared by controllable DGs gradually, which is implemented by the secondary control. Consequently, its outputs return to zero.

B. Distributed Control Laws

In this section, a systematic method is presented to derive a set of distributed control laws for agents, where only neighbors' information is needed. Furthermore, this set of control laws can be applied not only to the control of MGs, but also to their management by substituting a parameter in the control laws conveniently. Here, some terms are introduced first, and then an equation for power balance is given. Finally, a set of control laws is derived.

Assume there are n agents on the network. An adjacency matrix $A = [a_{ij}]_{n\times n}$ is defined to describe the relationships among agents, where a_{ij} will be one, if there is an outgoing edge from agents i to j. Otherwise, it is $a_{ij} = 0$. Next, a diagonal matrix $B = [b_{ii}]_{n\times n}$ is used to indicate the type of an agent, which means $b_{ii} = 1$, if the agent is a controllable agent. Otherwise, it is $b_{ii} = 0$. Finally, a diagonal matrix $D = [d_{ii}]_{n\times n}$ is defined, which represents the outdegree of an agent, where the outdegree is the number of outgoing edges of the agent. Therefore, we have

$$d_{ii} = \sum_{j=1}^{n} a_{ij}. \tag{1}$$

Moreover, to allow the sizes of matrices for the control laws to be equal, the number of agents is equal to that of DGs and that of loads. However, if the number of loads is greater than that of agents or DGs, a few loads nearby need to be considered as a large load and then it is connected to an agent. Conversely, if the number of loads is less than that of agents, some virtual loads with zero demand will be added to the MG in order to satisfy the requirement.

In this paper, it is deemed that the supply-demand balance maintains, if the change of outputs of all controllable DGs at two successive time steps plus the change of outputs of all uncontrollable DGs at two successive time steps is equal to that of the demand of all loads at two successive time steps,

$$\begin{cases} \sum\{B\cdot[P(t)-P(t-1)]\} = \sum[L^p(t)-L^p(t-1)] \\ \qquad\qquad -\sum\{(I-B)\cdot[P(t)-P(t-1)]\}, \\ \sum\{B\cdot[Q(t)-Q(t-1)]\} = \sum[L^q(t)-L^q(t-1)] \\ \qquad\qquad -\sum\{(I-B)\cdot[Q(t)-Q(t-1)]\}, \end{cases} \tag{2}$$

where $P(\cdot) = [p_i(\cdot)]_{n\times 1}$ and $Q(\cdot) = [q_i(\cdot)]_{n\times 1}$ are active and reactive outputs, while $L^p(\cdot) = [l_i^p(\cdot)]_{n\times 1}$ and $L^q(\cdot) = [l_i^q(\cdot)]_{n\times 1}$ are active and reactive load demand, and I is an $n\times n$ identity matrix.

Further, if the communication network G is given, a set of control laws will be derived as follows,

$$\begin{aligned} B\cdot P(t) &= W_p^T(t-1)\cdot[B\cdot P(t-1)] + U^T\cdot[L^p(t)-L^p(t-1)] \\ &\quad -V^T\cdot\{(I-B)\cdot[P(t)-P(t-1)]\} \\ &= W_p^T(t-1)\cdot[B\cdot P(t-1)] + U^T\cdot\Delta L^p - V^T\cdot[(I-B)\cdot\Delta P], \end{aligned} \tag{3}$$

where W_p, U and V are weighted matrices, while $(\cdot)^T$ denotes the transpose of a matrix. These weighted matrices are calculated as follows,

$$V = D^{-1}\cdot A, \tag{4}$$

$$U = (I-B)\cdot V + B, \tag{5}$$

$$W_p(t-1) = I - \mathrm{diag}(M_3\cdot\mathbf{1}_{n\times 1}) + M_3, \tag{6}$$

where

$$\begin{cases} M_1 = \mathrm{diag}[P(t-1)]\cdot B\cdot(A-I), \\ M_2 = \mathrm{diag}(X^p)\cdot\mathbf{1}_{n\times n}, \\ M_3 = \left|M_1\circ M_2^{\circ(-1)} - (M_1+M_1^T)\circ[(M_2+M_2^T)^{\circ(-1)}]\right|. \end{cases} \tag{7}$$

Here, $\mathbf{1}_{n\times 1}$ is a column vector whose all elements are one, $\mathrm{diag}(\cdot)$ denotes a function that creates an $n\times n$ diagonal matrix from an $n\times 1$ vector, and $[\cdot]^{-1}$ denotes the inverse of a matrix, while '$\circ$' represents the *Hadamard product* [35] and '$\circ(-1)$' is the *Hadamard inverse* [36]. Noting that if all "P" and "p" are replaced by "Q" and "q", the control laws for reactive power will be obtained, and $X = [x_i]_{n\times 1}$ is a vector, which can be substituted in terms of different purposes. For example, suppose $C^p = [c_i^p]_{n\times 1}$ and $C^q = [c_i^q]_{n\times 1}$

are the maximal active and reactive capacities of DGs. If $X^p = \max\{c_i^p | i \in \{1,2,\cdots,n\}\} \cdot \mathbf{1}_{n\times 1}$, then the outputs of all controllable DGs will be equal. Furthermore, if $X^p = C^p$, then the outputs of all controllable DGs will be proportional to their capacities. More details are given in Section IV.

C. Convergence analysis

In terms of (3), a set of control laws can be derived from a given communication network. If the control laws are applied by controllable agents to regulate the outputs of controllable DGs, the outputs of the V/F DG will return to zero, after instantaneously injecting or absorbing. Moreover, the outputs of controllable DGs will gradually converge to certain values satisfying the given requirements. In this section, theorems and a proposition are proven, which guarantee the convergence of the control laws. First, Theorem 1 is given as follows.

Theorem 1: Assume there is a directed communication network G with n agents over an MG, in which the kth agent is a partially controllable agent and other agents are controllable or uncontrollable. If controllable agents calculate the set points of controllable DGs in terms of the control laws (3), and regulate their outputs, the outputs of the partially controllable DG will be shared by controllable DGs, and (2) will always hold.

Proof: First, we prove the sum of elements of every row of a weighted matrix is one. According to (4), we have

$$V = D^{-1}\cdot A = \begin{bmatrix} \frac{a_{11}}{d_{11}} & \cdots & \frac{a_{1i}}{d_{11}} & \cdots & \frac{a_{1n}}{d_{11}} \\ \vdots & \ddots & \vdots & \vdots & \vdots \\ \frac{a_{i1}}{d_{ii}} & \cdots & \frac{a_{ii}}{d_{ii}} & \cdots & \frac{a_{in}}{d_{ii}} \\ \vdots & \vdots & \vdots & \ddots & \vdots \\ \frac{a_{n1}}{d_{nn}} & \cdots & \frac{a_{ni}}{d_{nn}} & \cdots & \frac{a_{nn}}{d_{nn}} \end{bmatrix}. \tag{8}$$

If summing up the ith row of V and applying (1), it yields

$$\sum_{j=1}^{n} v_{ij} = \frac{(a_{i1}+a_{i2}+\cdots a_{in})}{d_{ii}} = 1. \tag{9}$$

Similarly, $U = (I-B)\cdot V + B =$

$$\begin{bmatrix} \frac{a_{11}(1-b_{11})}{d_{11}}+b_{11} & \cdots & \frac{a_{1i}(1-b_{11})}{d_{11}} & \cdots & \frac{a_{1n}(1-b_{11})}{d_{11}} \\ \vdots & \ddots & \vdots & \vdots & \vdots \\ \frac{a_{i1}(1-b_{ii})}{d_{ii}} & \cdots & \frac{a_{ii}(1-b_{ii})}{d_{ii}}+b_{ii} & \cdots & \frac{a_{in}(1-b_{ii})}{d_{ii}} \\ \vdots & \vdots & \vdots & \ddots & \vdots \\ \frac{a_{n1}(1-b_{nn})}{d_{nn}} & \cdots & \frac{a_{ni}(1-b_{nn})}{d_{nn}} & \cdots & \frac{a_{nn}(1-b_{nn})}{d_{nn}}+b_{nn} \end{bmatrix}. \tag{10}$$

Summing up the ith row of U, we have

$$\sum_{j=1}^{n} u_{ij} = \frac{(a_{i1}+a_{i2}+\cdots a_{in})(1-b_{ii})}{d_{ii}} + b_{ii} = 1. \tag{11}$$

Finally, $W_p(t-1) = I - \mathrm{diag}(M_3\cdot\mathbf{1}_{n\times 1}) + M_3$ (See (12) for the full expansion.)

Summing up the ith row of W_p, we have

$$\begin{aligned} &\sum_{j=1}^{n} w_{ij}^p(t-1) = \\ &\left|\frac{a_{i1}b_{ii}p_i(t-1)}{x_i^p} - \frac{a_{i1}b_{ii}p_i(t-1)+a_{1i}b_{11}p_1(t-1)}{x_i^p+x_1^p}\right| + \cdots \\ &+1 - \sum_{j=1,j\neq i}^{n}\left|\frac{a_{ij}b_{ii}p_i(t-1)}{x_i^p} - \frac{a_{ij}b_{ii}p_i(t-1)+a_{ji}b_{jj}p_j(t-1)}{x_i^p+x_j^p}\right| \\ &+\cdots+\left|\frac{a_{in}b_{ii}p_i(t-1)}{x_i^p} - \frac{a_{in}b_{ii}p_i(t-1)+a_{ni}b_{nn}p_n(t-1)}{x_i^p+x_n^p}\right| = 1. \end{aligned} \tag{12a}$$

Next, we prove that (2) is satisfied. If both sides of the control laws (3) are summed up respectively, we have

$$\begin{aligned} &\sum B\cdot P(t) = \sum W_p^T\cdot[B\cdot P(t-1)] \\ &+\sum U^T\cdot[L^p(t)-L^p(t-1)] \\ &-\sum V^T\cdot\{(I-B)\cdot[P(t)-P(t-1)]\}, \\ &=[w_{11}^p+w_{12}^p+\cdots+w_{1n}^p]\cdot b_{11}\cdot p_1(t-1)+\cdots \\ &+[w_{k1}^p+w_{k2}^p+\cdots+w_{kn}^p]\cdot b_{kk}\cdot\gamma\cdot p_k(t-1)+\cdots \\ &+[w_{n1}^p+w_{n2}^p+\cdots+w_{nn}^p]\cdot b_{nn}\cdot p_n(t-1) \\ &+(u_{11}+u_{12}+\cdots+u_{1n})\cdot[l_1^p(t)-l_1^p(t-1)]+\cdots \\ &+(u_{k1}+u_{k2}+\cdots+u_{kn})\cdot[l_k^p(t)-l_k^p(t-1)]+\cdots \\ &+(u_{n1}+u_{n2}+\cdots+u_{nn})\cdot[l_n^p(t)-l_n^p(t-1)] \\ &+(v_{11}+v_{12}+\cdots+v_{1n})\cdot\{(1-b_{11})\cdot[-p_1(t)+p_1(t-1)]\}+\cdots \\ &+(v_{k1}+v_{k2}+\cdots+v_{kn})\cdot\{(1-b_{kk})\cdot\gamma\cdot[-p_k(t)+p_k(t-1)]\}+\cdots \\ &+(v_{n1}+v_{n2}+\cdots+v_{nn})\cdot\{(1-b_{nn})\cdot[-p_n(t)+p_n(t-1)]\}. \end{aligned} \tag{13}$$

Applying the results that the sum of a row of W_p, U or V is one to (13), it yields

$$\begin{aligned} &\sum B\cdot P(t) = \sum W_p^T\cdot[B\cdot P(t-1)] \\ &+\sum U^T\cdot[L^p(t)-L^p(t-1)] \\ &-\sum V^T\cdot\{(I-B)\cdot[P(t)-P(t-1)]\}, \\ &=b_{11}\cdot p_1(t-1)+\cdots+b_{kk}\cdot\gamma\cdot p_k(t-1)+\cdots+b_{nn}\cdot p_n(t-1) \\ &+[l_1^p(t)-l_1^p(t-1)]+\cdots+[l_k^p(t)-l_k^p(t-1)]+\cdots \\ &+[l_n^p(t)-l_n^p(t-1)]+(1-b_{11})\cdot[-p_1(t)+p_1(t-1)]+\cdots \\ &+(1-b_{kk})\cdot\gamma\cdot[-p_k(t)+p_k(t-1)]+\cdots \\ &+(1-b_{nn})\cdot[-p_n(t)+p_n(t-1)] \\ &=\sum B\cdot P(t-1)+\sum[L^p(t)-L^p(t-1)] \\ &-\sum\{(I-B)\cdot[P(t)-P(t-1)]\}. \end{aligned} \tag{14}$$

■

Observing the control laws (3), it can be found that if environmental conditions and load demand do not change, outputs of DGs and load demand at two successive time steps remain constant, i.e., $P(t) = P(t-1)$ and $L^p(t) = L^p(t-1)$. Thus, the control laws (3) is reduced to $B\cdot P(t) = W_p^T\cdot[B\cdot P(t-1)]$, which means iterations start and the outputs of controllable DGs are iteratively reassigned among them according to different X. For instance, as mentioned above, if $X^p = \max\{c_i^p | i\in\{1,2,\cdots,n\}\}\cdot\mathbf{1}_{n\times 1} = c^p\cdot\mathbf{1}_{n\times 1}$, then the

This article has been accepted for publication in a future issue of this journal, but has not been fully edited. Content may change prior to final publication. Citation information: DOI 10.1109/TSG.2018.2791398, IEEE Transactions on Smart Grid

$$W_p(t-1) = I - \mathrm{diag}(M_3 \cdot \mathbf{1}_{n\times 1}) + M_3 = \begin{bmatrix} 1-\sum_{j=2}^{n}\left|\frac{a_{1j}b_{11}p_1(t-1)}{x_1^p} - \frac{a_{1j}b_{11}p_1(t-1)+a_{j1}b_{jj}p_j(t-1)}{x_1^p+x_j^p}\right| & \cdots & \left|\frac{a_{1i}b_{11}p_1(t-1)}{x_1^p} - \frac{a_{1i}b_{11}p_1(t-1)+a_{i1}b_{ii}p_i(t-1)}{x_1^p+x_i^p}\right| & \cdots & \left|\frac{a_{1n}b_{11}p_1(t-1)}{x_1^p} - \frac{a_{1n}b_{11}p_1(t-1)+a_{n1}b_{nn}p_n(t-1)}{x_1^p+x_n^p}\right| \\ \vdots & \ddots & \vdots & \vdots & \vdots \\ \left|\frac{a_{i1}b_{ii}p_i(t-1)}{x_i^p} - \frac{a_{i1}b_{ii}p_i(t-1)+a_{1i}b_{11}p_1(t-1)}{x_i^p+x_1^p}\right| & \cdots & 1-\sum_{j=1,j\neq i}^{n}\left|\frac{a_{ij}b_{ii}p_i(t-1)}{x_i^p} - \frac{a_{ij}b_{ii}p_i(t-1)+a_{ji}b_{jj}p_j(t-1)}{x_i^p+x_j^p}\right| & \cdots & \left|\frac{a_{in}b_{ii}p_i(t-1)}{x_i^p} - \frac{a_{in}b_{ii}p_i(t-1)+a_{ni}b_{nn}p_n(t-1)}{x_i^p+x_n^p}\right| \\ \vdots & \vdots & \vdots & \ddots & \vdots \\ \left|\frac{a_{n1}b_{nn}p_n(t-1)}{x_n^p} - \frac{a_{n1}b_{nn}p_n(t-1)+a_{1n}b_{11}p_1(t-1)}{x_n^p+x_1^p}\right| & \cdots & \left|\frac{a_{ni}b_{nn}p_n(t-1)}{x_n^p} - \frac{a_{ni}b_{nn}p_n(t-1)+a_{in}b_{ii}p_i(t-1)}{x_n^p+x_i^p}\right| & \cdots & 1-\sum_{j=1}^{n-1}\left|\frac{a_{nj}b_{nn}p_n(t-1)}{x_n^p} - \frac{a_{nj}b_{nn}p_n(t-1)+a_{jn}b_{jj}p_j(t-1)}{x_n^p+x_j^p}\right| \end{bmatrix} \tag{12}$$

outputs of controllable DGs will be equal after iterations. More importantly, if the control laws (3) is applied, the supply-demand balance will never be broken during iterations, which means outputs reassigning among controllable DGs does not disturb the system, as shown in the following theorem.

Theorem 2: Assume there is a directed communication network G with n agents over an MG, in which the kth agent is a partially controllable agent and other agents are controllable or uncontrollable, and *environmental conditions and load demand do not change*. During iterations, if controllable agents calculate the set points of controllable DGs in terms of the control laws (3), and regulate their outputs, (2) will always hold.

Proof: If environmental conditions and load demand do not change, (2) and (3) are reduced to

$$\sum B \cdot P(t) = \sum B \cdot P(t-1), \tag{15}$$

and

$$B \cdot P(t) = W_p^T \cdot [B \cdot P(t-1)]. \tag{16}$$

Therefore, in this case, iterations start, i.e., outputs of controllable DGs are reassigned among them.

If both sides of (16) are summed up respectively, we have

$$\begin{aligned} &\sum B \cdot P(t) = \sum W_p^T \cdot [B \cdot P(t-1)] \\ &= [w_{11}^p + w_{12}^p + \cdots + w_{1n}^p] \cdot b_{11} \cdot p_1(t-1) + \cdots \\ &+ [w_{k1}^p + w_{k2}^p + \cdots + w_{kn}^p] \cdot b_{kk} \cdot \gamma \cdot p_k(t-1) + \cdots \\ &+ [w_{n1}^p + w_{n2}^p + \cdots + w_{nn}^p] \cdot b_{nn} \cdot p_n(t-1). \end{aligned} \tag{17}$$

Applying (12a), it yields

$$\begin{aligned} &\sum B \cdot P(t) = \sum W_p^T \cdot [B \cdot P(t-1)] \\ &= b_{11} \cdot p_1(t-1) + \cdots + b_{kk} \cdot \gamma \cdot p_k(t-1) + \cdots + b_{nn} \cdot p_n(t-1) \\ &= \sum B \cdot P(t-1). \end{aligned} \tag{18}$$

■

Furthermore, after a number of iterations, the outputs of controllable DGs will gradually converge to certain values satisfying the given targets, as shown in the following proposition.

Proposition 1: Assume there is a directed communication network G with $n = 14$ agents over an MG, where there are $m = 7$ controllable DGs, $\{\mathrm{DG}_i | i = 1, 3, 5, 6, 9, 11, 13\}$, and there is a partially controllable agent $k = 4$, as shown in Fig. 1. Let $X^p = c^p \cdot \mathbf{1}_{n\times 1}$ and the initial active outputs of controllable DGs is $[p_1(0), p_3(0), p_5(0), p_6(0), p_9(0), p_{11}(0), p_{13}(0)]^T = c^p \cdot [\theta, 2\theta, \cdots, 7\theta]^T$, where $c^p > 10^4$ and $0 < 7\theta \leq 1$. Assume that environmental conditions and load demand do not change. Applying the control laws (3), after 100 iterations, the difference between the maximal output and the average $\sum_i p_i(0)/m$ is less than or equal to $0.03c^p$. Therefore, the outputs of controllable DGs are approximately equal.

Proof: According to (3), the control laws for controllable agents are

$$\begin{aligned} p_1(t) &= w_{11}(t-1)p_1(t-1) + w_{31}(t-1)p_3(t-1) + w_{13,1}(t-1) \\ &\quad \cdot p_{13}(t-1) + \Delta l_1^p + 0.5\Delta l_2^p + 0.5\Delta l_{14}^p - 0.5\Delta p_2 - 0.5\Delta p_{14}; \\ p_3(t) &= w_{13}(t-1)p_1(t-1) + w_{33}(t-1)p_3(t-1) + w_{5,3}(t-1) \\ &\quad \cdot p_5(t-1) + 0.5\Delta l_2^p + \Delta l_3^p + 0.5\Delta l_4^p - 0.5\Delta p_2 - 0.5\gamma\Delta p_4; \\ &\vdots \end{aligned} \tag{19}$$

In this case, it is reduced to

$$\begin{aligned} p_1(t) &= w_{11}(t-1)p_1(t-1) + w_{31}(t-1)p_3(t-1) \\ &\quad + w_{13,1}(t-1)p_{13}(t-1); \\ p_3(t) &= w_{13}(t-1)p_1(t-1) + w_{33}(t-1)p_3(t-1) \\ &\quad + w_{5,3}(t-1)p_5(t-1); \\ &\vdots \end{aligned} \tag{20}$$

because environmental conditions and load demand do not change. Here, suppose θ takes the maximal value of $1/7$ due to $7\theta \leq 1$, so the average is $\sum_i p_i(0)/m = 0.57c^p$, to which the output of each controllable DG converges theoretically.

In terms of the control laws, controllable agents can calculate the set points of controllable DGs at the next time step. Therefore, after 50 and 100 iterations, the outputs of controllable DGs are listed respectively,

$$\begin{pmatrix} p_1(50) \\ p_3(50) \\ p_5(50) \\ p_6(50) \\ p_9(50) \\ p_{11}(50) \\ p_{13}(50) \end{pmatrix} = c^p \cdot \begin{pmatrix} 0.55 \\ 0.51 \\ 0.53 \\ 0.57 \\ 0.61 \\ 0.63 \\ 0.59 \end{pmatrix}, \quad \begin{pmatrix} p_1(100) \\ p_3(100) \\ p_5(100) \\ p_6(100) \\ p_9(100) \\ p_{11}(100) \\ p_{13}(100) \end{pmatrix} = c^p \cdot \begin{pmatrix} 0.56 \\ 0.54 \\ 0.55 \\ 0.57 \\ 0.59 \\ 0.60 \\ 0.58 \end{pmatrix}. \tag{21}$$

And the absolute values of the differences between the outputs

after 100 iterations and the average are

$$\left\|\begin{pmatrix} p_1(100) \\ p_3(100) \\ p_5(100) \\ p_6(100) \\ p_9(100) \\ p_{11}(100) \\ p_{13}(100) \end{pmatrix} - c^p \cdot \begin{pmatrix} 0.57 \\ 0.57 \\ 0.57 \\ 0.57 \\ 0.57 \\ 0.57 \\ 0.57 \end{pmatrix}\right\| = c^p \cdot \left\|\begin{pmatrix} 0.56-0.57 \\ 0.54-0.57 \\ 0.55-0.57 \\ 0.57-0.57 \\ 0.59-0.57 \\ 0.60-0.57 \\ 0.58-0.57 \end{pmatrix}\right\| = c^p \cdot \begin{pmatrix} 0.01 \\ 0.03 \\ 0.02 \\ 0 \\ 0.02 \\ 0.03 \\ 0.01 \end{pmatrix} \tag{22}$$

According to (22), it can be seen that the maximal deviation is $0.03c^p$. Thus, it is concluded that the outputs of controllable DGs are approximately equal. Finally, it also can be predicted that more iterations, less difference between the maximal output and the value in theory. ■

On the other hand, equal outputs of controllable DGs also can be obtained by the averaging algorithm for consensus, but during iterations the supply-demand balance will be broken, so that the outputs of the partially controllable DG will not be around zero, which means the system will be disturbed by outputs reassigning among controllable DGs. This is shown by the following theorem.

Theorem 3: Assume there is a directed communication network G with n agents over an MG, in which the kth agent is a partially controllable agent and other agents are controllable or uncontrollable, and *environmental conditions and load demand do not change*. During iterations, if controllable agents calculate the set points of controllable DGs in terms of the averaging algorithm for consensus, and regulate their outputs, (2) or (15) will not always hold. In other words, (2) or (15) will hold, if and only if the degrees of agents are identical.

Proof: According to the averaging algorithm for consensus, the output of a DG is the average of its neighbors' outputs and its own, e.g. $p_i(t) = \frac{a_{1i}}{d_{ii}} b_{11} p_1(t-1) + \frac{a_{2i}}{d_{ii}} b_{22} p_2(t-1) + \cdots + \frac{a_{ni}}{d_{ii}} b_{nn} p_n(t-1)$, which can be expressed in matrix as

$$B \cdot \begin{pmatrix} p_1(t) \\ \vdots \\ p_i(t) \\ \vdots \\ p_n(t) \end{pmatrix} = \begin{bmatrix} \frac{a_{11}}{d_{11}} & \cdots & \frac{a_{i1}}{d_{11}} & \cdots & \frac{a_{n1}}{d_{11}} \\ \vdots & \ddots & \vdots & \vdots & \vdots \\ \frac{a_{1i}}{d_{ii}} & \cdots & \frac{a_{ii}}{d_{ii}} & \cdots & \frac{a_{ni}}{d_{ii}} \\ \vdots & \vdots & \vdots & \ddots & \vdots \\ \frac{a_{1n}}{d_{nn}} & \cdots & \frac{a_{in}}{d_{nn}} & \cdots & \frac{a_{nn}}{d_{nn}} \end{bmatrix} \cdot B \cdot \begin{pmatrix} p_1(t-1) \\ \vdots \\ p_i(t-1) \\ \vdots \\ p_n(t-1) \end{pmatrix}. \tag{23}$$

If both sides of (23) are summed up respectively, we have

$$\begin{aligned} &\sum B \cdot P(t) \\ &= \left[\frac{a_{11}}{d_{11}} + \cdots + \frac{a_{1i}}{d_{ii}} + \cdots + \frac{a_{1n}}{d_{nn}}\right] \cdot b_{11} \cdot p_1(t-1) + \cdots \\ &+ \left[\frac{a_{k1}}{d_{11}} + \cdots + \frac{a_{ki}}{d_{ii}} + \cdots + \frac{a_{kn}}{d_{nn}}\right] \cdot b_{kk} \cdot \gamma \cdot p_k(t-1) + \cdots \\ &+ \left[\frac{a_{n1}}{d_{11}} + \cdots + \frac{a_{ni}}{d_{ii}} + \cdots + \frac{a_{nn}}{d_{nn}}\right] \cdot b_{nn} \cdot p_n(t-1). \end{aligned} \tag{24}$$

If $d_{ii} \neq d_{jj}, i, j \in \{1, 2, \cdots, n\}, i \neq j$, then $\sum B \cdot P(t) \neq \sum B \cdot P(t-1)$, i.e., (15) does not hold. If and only if the degrees of agents are identical, namely $d_{ii} = d_{jj}, i, j \in \{1, 2, \cdots, n\}, i \neq j$, and (1) is applied, (24) is changed to

$$\begin{aligned} \sum B \cdot P(t) &= b_{11} \cdot p_1(t-1) + \cdots + b_{kk} \cdot \gamma \cdot p_k(t-1) + \cdots \\ &+ b_{nn} \cdot p_n(t-1) = \sum B \cdot P(t-1). \end{aligned} \tag{25}$$

In this case, (15) holds. ■

III. Microgrid System Architecture and Setup

For simulations, an MG with 14 DGs and 14 loads is established in MATLAB/Simulink, where there are seven controllable DGs implemented by ideal DC voltage sources V_{dc} [37], six uncontrollable DGs by PVs and WTs, and a partially controllable DG by a BESS, and all DGs connect to the buses through inverters. It is worth noting that in this paper PQ control and V/F control are implemented by inverters, but not by DGs themselves. Moreover, controllable DGs, $\{\text{DG}_i | i = 1, 3, 5, 6, 9, 11, 13\}$, work in PQ control mode, while uncontrollable DGs, $\{\text{DG}_i | i = 2, 7, 8, 10, 12, 14\}$, in maximum power point tracking (MPPT) control mode and the partially controllable DG, DG_4, in V/F control mode. Also, physical constraints of these DGs are considered. For example, the maximal capacities and the minimum of DGs cannot be exceeded, even if the set points are greater than the maximal capacities or less than zero. Furthermore, the instantaneous output of the BESS is limited and there is a capacity constraint, when the BESS charges or discharges.

In all simulations, no reactive power is produced by uncontrollable DGs in order to test the performance of the control laws for reactive power dispatch of controllable DGs, while the line voltage and the frequency in the system are set at 380 V and 50 Hz, respectively. Also, the line losses are considered, when the line impedance is set at $0.169 + j0.07$ Ω/km. Generally speaking, in a small islanded MG, the line losses are not large because the lengths of power lines between two DGs are not very long. Therefore, in our model, it is considered that the line losses are compensated by the outputs of the V/F DG first, and then the outputs of the V/F DG are shared by controllable DGs by means of the derived control laws. Furthermore, initially, the MG system works in a balanced state. In Summary, these parameters and setups of DGs and loads are listed in Table I.

TABLE I
Setup and parameters of DGs and loads

Sources	Capacities	Control	Load	Max. Demand
DG_1	50 kW, 40 kVar	PQ	Load_1	20 kW, 0 kVar
DG_2	30 kW, 0 kVar	MPPT	Load_2	35 kW, 0 kVar
DG_3	60 kW, 25 kVar	PQ	Load_3	10 kW, 20 kVar
DG_4	30 Ah	V/F	Load_4	30 kW, 0 kVar
DG_5	55 kW, 20 kVar	PQ	Load_5	20 kW, 20 kVar
DG_6	65 kW, 30 kVar	PQ	Load_6	10 kW, 10 kVar
DG_7	50 kW, 0 kVar	MPPT	Load_7	20 kW, 0 kVar
DG_8	35 kW, 0 kVar	MPPT	Load_8	30 kW, 15 kVar
DG_9	45 kW, 38 kVar	PQ	Load_9	40 kW, 10 kVar
DG_{10}	45 kW, 0 kVar	MPPT	Load_{10}	20 kW, 15 kVar
DG_{11}	70 kW, 28 kVar	PQ	Load_{11}	15 kW, 20 kVar
DG_{12}	50 kW, 0 kVar	MPPT	Load_{12}	20 kW, 0 kVar
DG_{13}	40 kW, 35 kVar	PQ	Load_{13}	40 kW, 10 kVar
DG_{14}	40 kW, 0 kVar	MPPT	Load_{14}	30 kW, 0 kVar

This article has been accepted for publication in a future issue of this journal, but has not been fully edited. Content may change prior to final publication. Citation information: DOI 10.1109/TSG.2018.2791398, IEEE Transactions on Smart Grid

Throughout simulations, the outputs of PVs and WTs are shown in Fig. 2, while the load demand is scheduled as follows

- t = 1.5 s: Load_5 and Load_{14} are cut from the MG,
- t = 3 s: Load_5 and Load_{14} are connected to the MG.

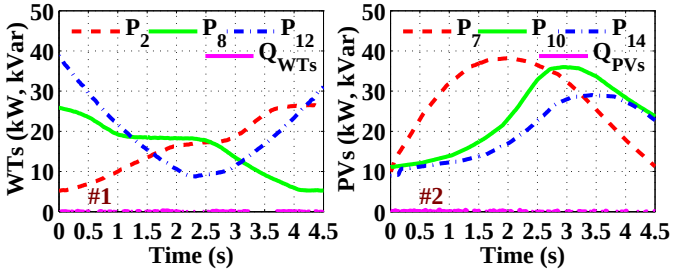

Fig. 2. Active and reactive power outputs of PVs and WTs.

Moreover, in this paper, *asynchronous communication* is adopted to transmit information among agents on a communication network, which is an efficient way to reduce communication traffic. Suppose there is a threshold $\Omega \geq 0$. If an agent i finds that the absolute value of the difference between the previous and the present values is greater than or equal to Ω, it will send the information to its neighbor j. On the other hand, if an agent does not receive any information from a neighbor, the previously received value will be used to calculate the set points. In this way, the number of information transmission is decreased significantly. In simulations, the threshold Ω_1 for information transmission is set at 1500, while Ω_2 is zero. In other words, the power values for uncontrollable DGs and those load demand are transmitted to controllable agents, if Ω_1 is triggered, while the values of set points calculated by controllable agents are exchanged among controllable agents, if Ω_2 is triggered, so as to satisfy the given requirements faster.

IV. Results

To evaluate the performance of the distributed method for the control and management of MGs, eight cases are designed. The first case focuses on the equal outputs of controllable DGs, while the second one on proportional outputs of controllable DGs to their capacities. The third focuses on energy management, where the near optimal incremental costs are obtained. The fourth, the fifth, the sixth and the seventh investigate the impacts of different thresholds, time delays, different topologies and link failures on the system performance, respectively. Finally, our results are compared with those obtained by the averaging algorithm for consensus. All of cases are carried out, when both load demand and environmental conditions fluctuate.

A. Case 1: Equal outputs of controllable DGs

According to the proposed method, the outputs of controllable DGs can satisfy the given requirements by substituting the parameter X. If the parameter $X^p = \max(C^p) \cdot \mathbf{1}_{n\times 1} = (7 \times 10^4) \cdot \mathbf{1}_{n\times 1}$ and $X^q = (4 \times 10^4) \cdot \mathbf{1}_{n\times 1}$, equal outputs of controllable DGs will be obtained. Following the settings mentioned in Section III, simulations are carried out and results are shown in Fig. 3.

Fig. 3(#4) is the frequency of the system, while (#5) is the line voltage, where we can see that they mostly change slightly except the moments when load demand fluctuates dramatically. However, even in those extreme moments, the system still works well, and the outputs of the V/F DG (DG_4) return zero after injecting or absorbing power instantaneously, as it is desired. Furthermore, from Fig. 3(#1) and (#2), it can be found that the active power outputs of controllable DGs are almost equal throughout the simulation, so do the reactive power outputs, which means the outputs of controllable DGs converge to a value quickly.

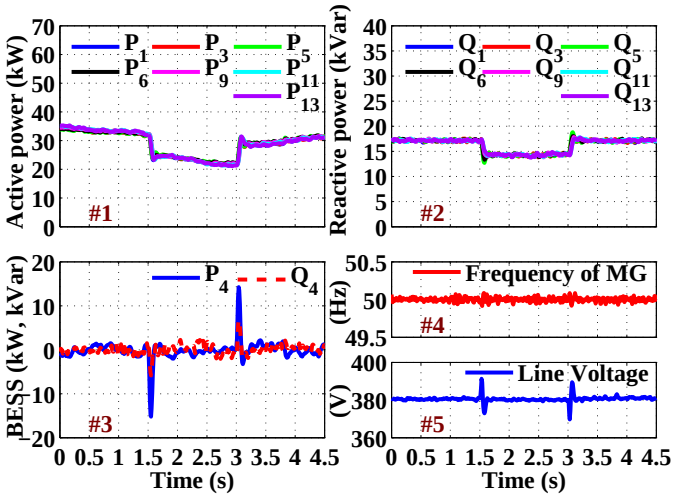

Fig. 3. Simulation results of equal outputs of controllable DGs. (#1) and (#2) are the active and reactive outputs of controllable DGs, while (#3) is the outputs of the partially controllable DG. (#4) and (#5) are the frequency and the line voltage.

B. Case 2: Proportional outputs of controllable DGs to their capacities

In this section, it is shown that how to select the parameter X in the control laws (3) makes the outputs of controllable DGs are proportional to their capacities. As is mentioned, if $X^p = C^p$ and $X^q = C^q$, the proportional outputs will be achieved. The simulation results are obtained, when both load demand and environmental conditions fluctuate, and other settings follow those in Section III.

As shown in Fig. 4, the results are very similar to those in Case 1, which also means the control laws (3) still can maintain the system stable, after X is replaced by other values. Moreover, the outputs of controllable DGs satisfy the requirements of proportional outputs, as shown in Fig. 4(#1) and (#2), where α_i and β_i are the proportions of the active and reactive power outputs of controllable DG_i to its capacities, respectively. Comparing with the results in Case 1, the fluctuations of the curves of proportions last a little longer after load demand changes significantly, which indicates that more iterations are needed to reach the convergence. Further, analyzing the weighted matrix W, we can find that the non-diagonal elements are the difference of power among agents in

Case 1, while those are the difference of proportions of outputs to capacities in this case. Thus, by iterations, W converges to an identity, and at the same time outputs of controllable DGs in Case 1 or the proportions of their outputs to capacities in Case 2 converge the same value gradually.

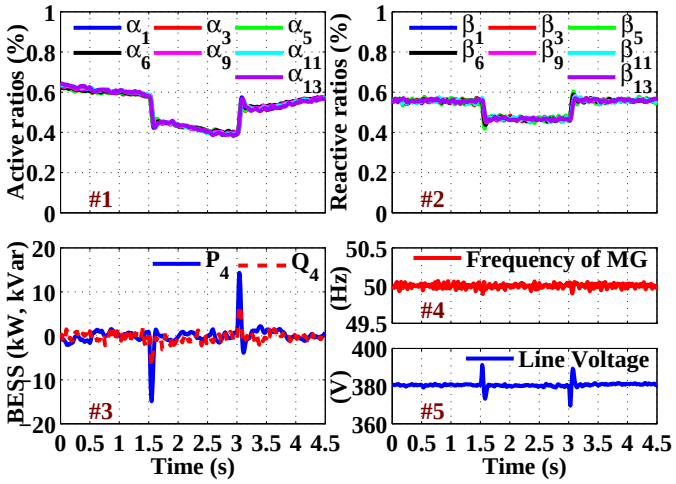

Fig. 4. Simulation results of proportional outputs of controllable DGs to their capacities. (#1) and (#2) are the proportions of the active and reactive power outputs of controllable DGs to its capacity, while (#3) is the outputs of the partially controllable DG. (#4) and (#5) are the frequency and the line voltage.

C. Case 3: Energy management: the optimal incremental cost

As mentioned above, the method can be used not only to control an MG, but also to manage the MG still by substituting the parameter X. As is known, the cost function is often written as $F_i(p_i) = \rho_i p_i^2 + \xi_i p_i + \eta_i$, where nonnegative ρ_i, ξ_i, and η_i are the cost coefficients that are listed in Table II. So, the incremental cost ϕ_i is the partial derivative of $F_i(\cdot)$, namely,

$$\phi_i = 2\rho_i p_i + \xi_i = \frac{p_i + \xi_i/2\rho_i}{1/2\rho_i} = \frac{p_i'}{x_i^p}, \tag{26}$$

and it is well known that the optimal incremental costs without constraints of DG capacities will be obtained, if the incremental costs of all controllable DGs are equal [38], also known as the equal incremental cost criterion.

TABLE II
COST PARAMETERS OF CONTROLLABLE DGS

Sources	ρ_i	ξ_i	η_i
DG_1	0.059	6.71	80
DG_3	0.047	7.08	56
DG_5	0.066	6.29	43
DG_6	0.031	7.53	35
DG_9	0.069	4.57	48
DG_{11}	0.038	5.86	91
DG_{13}	0.074	5.43	65

Therefore, to reach the optimal incremental costs, the control laws (3) is changed to

$$\begin{aligned} B \cdot P(t) = {} & W_{p'}^T(t-1) \cdot [B \cdot P'(t-1)] + U^T \cdot \Delta L^P \\ & - V^T \cdot [(I-B) \cdot \Delta P] - B \cdot [P(t-1) + \frac{\boldsymbol{\xi}}{2\boldsymbol{\rho}}], \end{aligned} \tag{27}$$

where $P'(t-1) = [p_i'(t-1)]_{n\times 1} = [p_i(t-1) + \xi_i/2\rho_i]_{n\times 1}$, $X^p = [x_i^p]_{n\times 1} = [1/2\rho_i]_{n\times 1}$ and $M_1 = \mathrm{diag}[P'(t-1)] \cdot B \cdot (A-I)$, while $\boldsymbol{\xi} = [\xi_i]_{n\times 1}$ and $\boldsymbol{\rho} = [\rho_i]_{n\times 1}$. Thus, an non-diagonal element of the matrix with dynamic weights $W_{p'}(t-1)$ should be

$$w_{ij}(t-1) = \left| \frac{p_i'}{x_i^p} - \frac{p_i' + p_j'}{x_i^p + x_j^p} \right|, \tag{28}$$

if there is an edge between agents i and j.

Generally speaking, the costs of PV generation, WT generation and reactive power generation are not considered [21], so only active power of controllable DGs are regulated according to (27), while reactive power of controllable DGs is still proportional to their capacities. Other settings follow those in Section III.

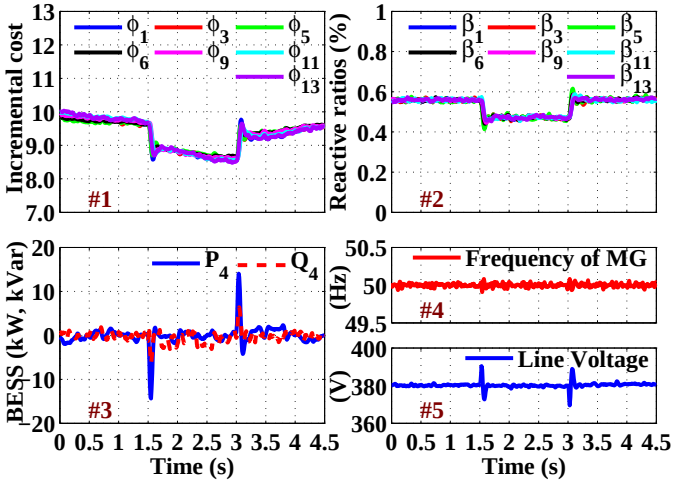

Fig. 5. Simulation results of the optimal incremental cost. (#1) is the incremental costs of controllable DGs, and (#2) is the proportions of the reactive power outputs of controllable DGs to its reactive capacity, while (#3) is the outputs of the partially controllable DG. (#4) and (#5) are the frequency and the line voltage.

Applying (27) to regulate the active power of controllable DGs, the simulation results of the economic dispatch problem are shown in Fig. 5, where Fig. 5(#1) is the incremental costs ϕ_i. It can be seen that the incremental costs of all controllable DGs are almost the same, which means the near optimal incremental costs are obtained.

D. Case 4: Impacts of the Threshold Ω_1 on the Performance When Both Environmental Conditions and Load Demand Fluctuate

To reduce the number of communications, in this paper asynchronous communication is adopted, where whether information transmission occurs or not depends on the threshold Ω_1. To evaluate the impacts of the threshold on the performance of our method, simulations are carried out under different thresholds, Ω_1=1000, 2000, 3000, when other settings follow those in Case 2. Simulation results are shown in Fig. 6.

From Fig. 6, it can be seen that the proportions of outputs of controllable DGs to their capacities are almost equal under different thresholds. Moreover, the voltage and the frequency are always around the prescribed values except the

This article has been accepted for publication in a future issue of this journal, but has not been fully edited. Content may change prior to final publication. Citation information: DOI 10.1109/TSG.2018.2791398, IEEE Transactions on Smart Grid

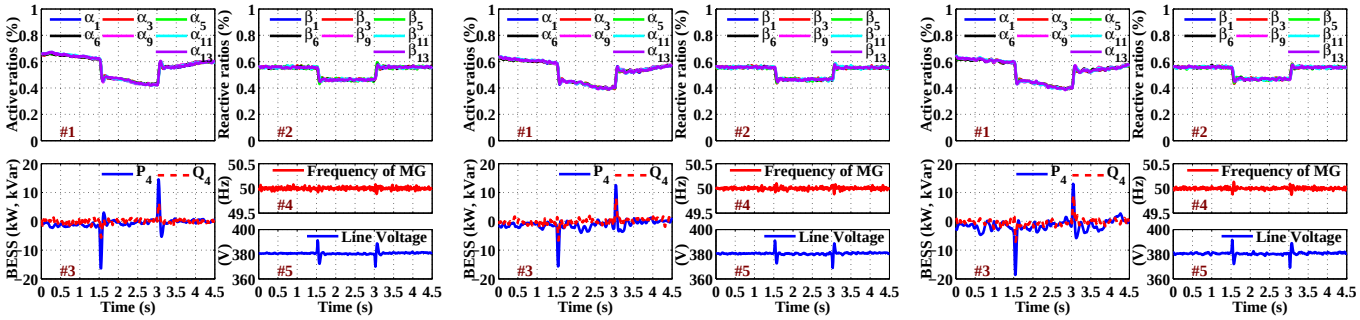

Fig. 6. Simulation results of proportional outputs of controllable DGs to their capacities under different thresholds. (a) Ω_1 = 1000. (b) Ω_1 = 2000. (c) Ω_1 = 3000. (#1) and (#2) are the proportions of the active and reactive power outputs of controllable DGs to its capacity, while (#3) is the outputs of the partially controllable DG. (#4) and (#5) are the frequency and the line voltage.

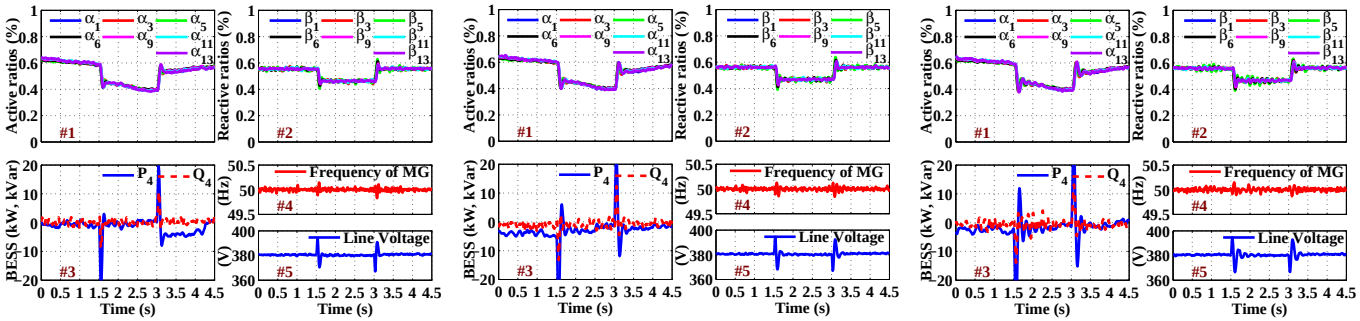

Fig. 7. Simulation results of proportional outputs of controllable DGs to their capacities, when time delays occur. (a) ω = 10 ms. (b) ω = 20 ms. (c) ω = 30 ms. (#1) and (#2) are the proportions of the active and reactive power outputs of controllable DGs to its capacity, while (#3) is the outputs of the partially controllable DG. (#4) and (#5) are the frequency and the line voltage.

load demand fluctuates dramatically, which means the system runs well. However, with the increase of the threshold, the time between two information transmissions also increases, which decreases the number of communications significantly, but causes the outputs of the BESS cannot be shared by controllable DGs quickly, namely returning to zero fast. This is why the fluctuation of the outputs of the BESS at Ω_1=1000 is much smaller than that at Ω_1=3000, as shown in Fig 6(a)(#3) and (c)(#3).

E. Case 5: Impacts of Time Delays on the Performance of the System

In a real communication system, time delays occur possibly due to data congestion. In this section, how time delays affect the system performance is discussed, since the communication network plays an important role in our method. During simulations, both environmental conditions and load demand fluctuate, where the settings follow those in Case 2, while a fixed time delay ω is adopted, when information is transmitted among agents.

Different time delays are applied to test the method, and simulation results are shown in Fig. 7, which are obtained at ω = 10, 20 and 30 ms, respectively. From Fig. 7, it can be seen that the outputs of controllable DGs are still proportional to their capacities, but the fluctuations of curves increase with the rise of ω. Compared with those without time delays, the time for fluctuations of voltages lasts longer, when a bigger time delay occurs, because agents cannot receive latest information and take effective actions to respond the changes of the system.

F. Case 6: The Topologies of Communication Networks versus the Performance of the System

To test the performance of the system on different communication networks, a communication network with more edges, $G_1(V, E)$, is designed by adding two edges from the uncontrollable agent 2 to the controllable agent 6 and from the uncontrollable agent 14 to the controllable agent 9, and two edges between the controllable agent 5 and the controllable agent 13 and between the controllable agent 9 and the controllable agent 13, as shown in Fig. 8. All other settings follow those in Case 1.

Fig. 9 is the simulation results on the new network $G_1(V, E)$, when both environmental conditions and load demand fluctuate over time. Compared with the results on $G(V, E)$ in Case 1, it can be found that almost the same results are obtained, although the difference among outputs of DGs is smaller. This is because more edges are added so that more information is exchanged. However, the large scale behavior of the curves of the outputs, the voltage and the frequency is not strongly associated with the topologies of networks, which offers a way

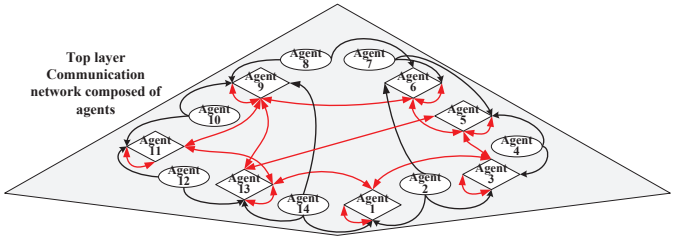

Fig. 8. The topology of a communication network, $G_1(V, E)$.

without many constraints to design communication networks.

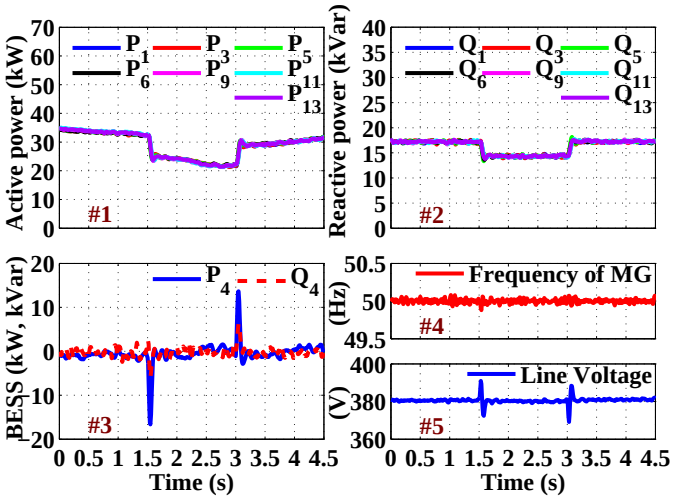

Fig. 9. Simulation results of equal outputs of controllable DGs on a different communication network $G_1(V, E)$. (#1) and (#2) are the active and reactive outputs of controllable DGs, while (#3) is the outputs of the partially controllable DG. (#4) and (#5) are the frequency and the line voltage.

G. Case 7: The link failures versus the Performance of the System

The previous case shows that the structures of communication networks do not affect the performance largely, but how link failures affect the system is still needed to be investigated. At the beginning, the network $G_1(V, E)$ is applied, while at t = 2.5 s four links fail, i.e., links between the agent 2 and the agent 6, the agent 14 and the agent 9, the agent 5 and the agent 13, the agent 9 and the agent 13 are broken. All other settings follow those in Case 1.

Under these settings, the simulation results are shown in Fig. 10. After link failures, if compared with the results in Case 6 (Fig. 9), there are almost no differences between the results. There are two main reasons. First, if there are no isolated agents on the communication network, our method will always work, even if links fail, for information still can be exchanged among agents. Second, information transmission does not occur frequently due to asynchronous communication, so link failures do not influence the performance significantly. Therefore, only if the communication network is connected, the targets of control and management will be achieved.

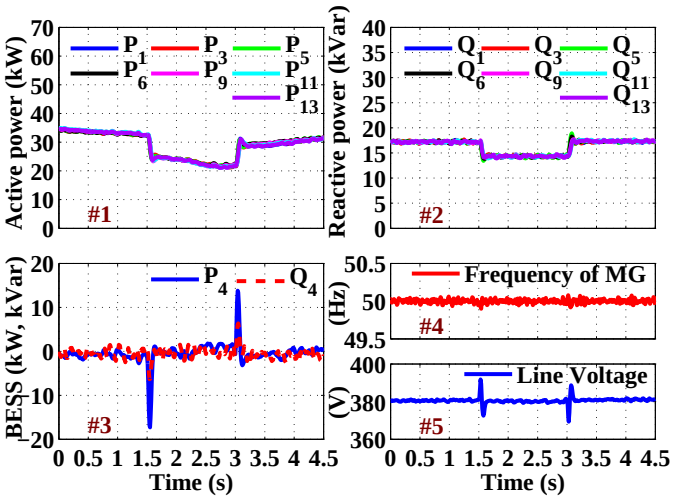

Fig. 10. Simulation results of link failures on the network $G_1(V, E)$. (#1) and (#2) are the active and reactive outputs of controllable DGs, while (#3) is the outputs of the partially controllable DG. (#4) and (#5) are the frequency and the line voltage.

H. Case 8: Comparison with averaging algorithm for consensus

The averaging algorithm for consensus is widely used as a distributed secondary method for the control and management of MGs. In this section, the performance of the averaging algorithm for consensus is compared with that of our method. In simulations, the communication network $G_1(V, E)$ with different degrees is adopted, and other settings follow those in Case 1.

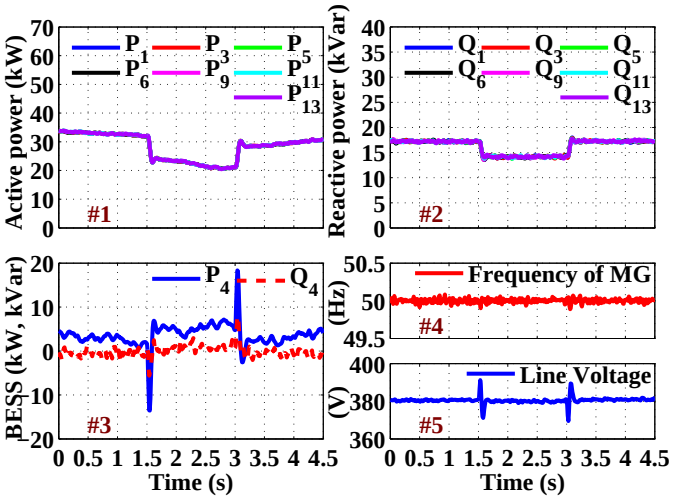

Fig. 11. Simulation results of equal outputs of controllable DGs, when the averaging algorithm for consensus is used. (#1) and (#2) are the active and reactive outputs of controllable DGs, while (#3) is the outputs of the partially controllable DG. (#4) and (#5) are the frequency and the line voltage.

The simulation results are shown in Fig. 11. Compared with the results in Case 6 (Fig. 9), it can be found that the outputs of DGs, the voltage and the frequency look similar. However, focusing on the outputs of the BESS (the V/F DG) that provide the system losses in order to maintain the frequency and

voltage constant in the system, we can see in Fig. 11(#3) the outputs of the BESS do not return to zero after fluctuations and remain at a value greater than zero during iterations, when the averaging algorithm for consensus is used. This is because the sum of the power outputs of controllable DGs before and after iterations is not equal, which indicates the supply-demand balance is broken during iterations, as stated by Theorem 3. On the other hand, in Fig. 9(#3), the outputs of the BESS is always around zero by our method.

V. Conclusion

We have proposed a distributed and networked method for control and management of MGs, which is a two layer model, where the top layer is a communication network composed of agents, while the bottom layer is the MG composed of DGs. Through the links between two layers, agents can acquire information from DGs and loads. Moreover, they can transmit this information to neighbors on the network. To deal with the information, a set of distributed control laws for controllable agents are derived from any given communication network by a systematic method. This method offers unified steps to achieve different targets by substituting a parameter in the control laws, where the control laws with dynamic weights reassign outputs of DGs in order to reach different targets iteratively. Moreover, during iterations, the control laws never break the system balance and do not disturb the system when outputs reassigning among controllable DGs. Further, theorems and a proposition are proved, which show that the control laws can guarantee that the outputs of controllable DGs satisfy a number of given requirements iteratively.

Different simulations are carried out, which show that equal outputs, proportional outputs and the near optimal incremental cost are obtained by substituting the parameter X. Moreover, our method is not strongly associated with the topologies of communication networks, so there are not many constraints for the network design. Compared with the results obtained by the averaging algorithm for consensus under the same settings, our results show that the supply-demand balance is never broken during iterations. In summary, our method offers a straightforward way to reach different targets of control and management of MGs by simply substituting a parameter in the distributed control laws with dynamic weights. For future work, analysing the rate of convergence in theory and more accurate voltage regulation are significant questions.

Acknowledgment

This work was supported in part by the National Natural Science Foundation of China (Grant No. 61105125 & No. 51177177), National "111" Project of China (Grant No. B08036) and Basic and Frontier Research Project of Chongqing (Grant No. cstc2017jcyjAX0037).

References

[1] D. Abbott, "Keeping the energy debate clean: How do we supply the world's energy needs?" *Proc. IEEE*, vol. 98, no. 1, pp. 42–66, Jan 2010.

[2] ——, "Nuclear power: Game over," *Australian Quarterly*, vol. 87, no. 4, pp. 8–16, 2016.

[3] R. H. Lasseter and P. Paigi, "Microgrid: a conceptual solution," in *IEEE 35th Annual Power Electronics Specialists Conference*, vol. 6, June 2004, pp. 4285–4290.

[4] R. Lasseter, "Smart distribution: Coupled microgrids," *Proc. IEEE*, vol. 99, no. 6, pp. 1074–1082, June 2011.

[5] J. M. Guerrero, J. C. Vasquez, J. Matas, L. G. de Vicua, and M. Castilla, "Hierarchical control of droop-controlled ac and dc microgrids - a general approach toward standardization," *IEEE Trans. Ind. Electron.*, vol. 58, no. 1, pp. 158–172, Jan 2011.

[6] A. Bidram and A. Davoudi, "Hierarchical structure of microgrids control system," *IEEE Trans. Smart Grid*, vol. 3, no. 4, pp. 1963–1976, Dec 2012.

[7] J. M. Guerrero, M. Chandorkar, T. Lee, and P. C. Loh, "Advanced control architectures for intelligent microgrids—Part I: Decentralized and hierarchical control," *IEEE Trans. Ind. Electron.*, vol. 60, no. 4, pp. 1254–1262, April 2013.

[8] Y. Han, H. Li, P. Shen, E. A. A. Coelho, and J. M. Guerrero, "Review of active and reactive power sharing strategies in hierarchical controlled microgrids," *IEEE Trans. Power Electron.*, vol. 32, no. 3, pp. 2427–2451, March 2017.

[9] K. T. Tan, X. Y. Peng, P. L. So, Y. C. Chu, and M. Z. Q. Chen, "Centralized control for parallel operation of distributed generation inverters in microgrids," *IEEE Trans. Smart Grid*, vol. 3, no. 4, pp. 1977–1987, Dec 2012.

[10] T. Hong and F. D. Leon, "Centralized unbalanced dispatch of smart distribution dc microgrid systems," *IEEE Trans. Smart Grid*, vol. PP, no. 99, pp. 1–1, 2016.

[11] N. L. Díaz, A. C. Luna, J. C. Vasquez, and J. M. Guerrero, "Centralized control architecture for coordination of distributed renewable generation and energy storage in islanded ac microgrids," *IEEE Trans. Power Electron.*, vol. 32, no. 7, pp. 5202–5213, July 2017.

[12] M. Karimi, P. Wall, H. Mokhlis, and V. Terzija, "A new centralized adaptive underfrequency load shedding controller for microgrids based on a distribution state estimator," *IEEE Trans. Power Del.*, vol. 32, no. 1, pp. 370–380, Feb 2017.

[13] J. Simpson-Porco, Q. Shafiee, F. Dorfler, J. Vasquez, J. Guerrero, and F. Bullo, "Secondary frequency and voltage control of islanded microgrids via distributed averaging," *IEEE Trans. Ind. Electron.*, vol. 62, no. 11, pp. 7025–7038, Nov 2015.

[14] N. Yorino, Y. Zoka, M. Watanabe, and T. Kurushima, "An optimal autonomous decentralized control method for voltage control devices by using a multi-agent system," *IEEE Trans. Power Syst.*, vol. 30, no. 5, pp. 2225–2233, Sept 2015.

[15] X. Lu, X. Yu, J. Lai, Y. Wang, and J. M. Guerrero, "A novel distributed secondary coordination control approach for islanded microgrids," *IEEE Trans. Smart Grid*, 2016, DOI: 10.1109/TSG.2016.2618120.

[16] Q. Li, C. Peng, M. Chen, F. Chen, W. Kang, J. M. Guerrero, and D. Abbott, "Networked and distributed control method with optimal power dispatch for islanded microgrids," *IEEE Trans. Ind. Electron.*, vol. 64, no. 1, pp. 493–504, Jan 2017.

[17] J. Yu, C. Dou, and X. Li, "MAS-based energy management strategies for a hybrid energy generation system," *IEEE Trans. Ind. Electron.*, vol. 63, no. 6, pp. 3756–3764, June 2016.

[18] C. Dou, D. Yue, X. Li, and Y. Xue, "Mas-based management and control strategies for integrated hybrid energy system," *IEEE Trans. Ind. Informat.*, vol. 12, no. 4, pp. 1332–1349, Aug 2016.

[19] Y. S. Kim, E. S. Kim, and S. I. Moon, "Distributed generation control method for active power sharing and self-frequency recovery in an islanded microgrid," *IEEE Trans. Power Syst.*, vol. 32, no. 1, pp. 544–551, Jan 2017.

[20] P. Shamsi, H. Xie, A. Longe, and J. Y. Joo, "Economic dispatch for an agent-based community microgrid," *IEEE Trans. Smart Grid*, vol. 7, no. 5, pp. 2317–2324, Sept 2016.

[21] F. Chen, M. Chen, Q. Li, K. Meng, Y. Zheng, J. M. Guerrero, and D. Abbott, "Cost-based droop schemes for economic dispatch in islanded microgrids," *IEEE Trans. Smart Grid*, vol. 8, no. 1, pp. 63–74, Jan 2017.

[22] J. Schiffer, T. Seel, J. Raisch, and T. Sezi, "Voltage stability and reactive power sharing in inverter-based microgrids with consensus-based distributed voltage control," *IEEE Trans. Control Syst. Technol.*, vol. 24, no. 1, pp. 96–109, Jan 2016.

[23] L. Meng, X. Zhao, F. Tang, M. Savaghebi, T. Dragicevic, J. C. Vasquez, and J. M. Guerrero, "Distributed voltage unbalance compensation in islanded microgrids by using a dynamic consensus algorithm," *IEEE Trans. Power Electron.*, vol. 31, no. 1, pp. 827–838, Jan 2016.

[24] L. Meng, T. Dragicevic, J. Roldan-Perez, J. C. Vasquez, and J. M. Guerrero, "Modeling and sensitivity study of consensus algorithm-based

distributed hierarchical control for dc microgrids," *IEEE Trans. Smart Grid*, vol. 7, no. 3, pp. 1504–1515, May 2016.
[25] Q. Sun, R. Han, H. Zhang, J. Zhou, and J. M. Guerrero, "A multiagent-based consensus algorithm for distributed coordinated control of distributed generators in the energy internet," *IEEE Trans. Smart Grid*, vol. 6, no. 6, pp. 3006–3019, Nov 2015.
[26] A. Q. Huang, M. L. Crow, G. T. Heydt, J. P. Zheng, and S. J. Dale, "The future renewable electric energy delivery and management (freedm) system: The energy internet," *Proc. IEEE*, vol. 99, no. 1, pp. 133–148, Jan 2011.
[27] S. Zuo, A. Davoudi, Y. Song, and F. L. Lewis, "Distributed finite-time voltage and frequency restoration in islanded ac microgrids," *IEEE Trans. Ind. Electron.*, vol. 63, no. 10, pp. 5988–5997, Oct 2016.
[28] Y. Xu and Z. Li, "Distributed optimal resource management based on the consensus algorithm in a microgrid," *IEEE Trans. Ind. Electron.*, vol. 62, no. 4, pp. 2584–2592, April 2015.
[29] J. Tsitsiklis, D. Bertsekas, and M. Athans, "Distributed asynchronous deterministic and stochastic gradient optimization algorithms," *IEEE Trans. Autom. Control*, vol. 31, no. 9, pp. 803–812, Sep 1986.
[30] A. Jadbabaie, J. Lin, and A. S. Morse, "Coordination of groups of mobile autonomous agents using nearest neighbor rules," *IEEE Trans. Autom. Control*, vol. 48, no. 6, pp. 988–1001, June 2003.
[31] R. Olfati-Saber, J. A. Fax, and R. M. Murray, "Consensus and cooperation in networked multi-agent systems," *Proc. IEEE*, vol. 95, no. 1, pp. 215–233, March 2007.
[32] L. Guo, W. Liu, X. Li, Y. Liu, B. Jiao, W. Wang, C. Wang, and F. Li, "Energy management system for stand-alone wind-powered-desalination microgrid," *IEEE Trans. Smart Grid*, vol. 7, no. 2, pp. 1079–1087, March 2016.
[33] B. Zhao, X. Zhang, J. Chen, C. Wang, and L. Guo, "Operation optimization of standalone microgrids considering lifetime characteristics of battery energy storage system," *IEEE Trans. Sustainable Energy*, vol. 4, no. 4, pp. 934–943, Oct 2013.
[34] B. Zhao, X. Zhang, and J. Chen, "Integrated microgrid laboratory system," *IEEE Trans. Power Syst.*, vol. 27, no. 4, pp. 2175–2185, Nov 2012.
[35] B.-Y. Wang, X. Zhang, and F. Zhang, "On the hadamard product of inverse m-matrices," *Linear Algebra and its Applications*, vol. 305, no. 1-3, pp. 23–31, 2000.
[36] R. Reams, "Hadamard inverses, square roots and products of almost semidefinite matrices," *Linear Algebra and its Applications*, vol. 288, pp. 35–43, 1999.
[37] R. Majumder, B. Chaudhuri, A. Ghosh, R. Majumder, G. Ledwich, and F. Zare, "Improvement of stability and load sharing in an autonomous microgrid using supplementary droop control loop," *IEEE Trans. Power Syst.*, vol. 25, no. 2, pp. 796–808, May 2010.
[38] A. J. Wood, B. F. Wollenberg, and G. B. Sheblé, *Power Generation, Operation, and Control*, 3rd ed. Wiley, 2013.

Qiang Li received the Ph.D. degree in electrical engineering from Zhejiang University, Hangzhou, China, in 2009. He was a Post-Doctoral Fellow with Chongqing University from 2009 to 2012 and a Visiting Post-Doctoral Scholar with the University of Adelaide, Adelaide, SA, Australia, from 2011 to 2012. He is currently an Associate Professor with Chongqing University. His current research interests include networked control systems, optimization of microgrids, evolutionary dynamics.

Congbo Peng received the B.S. degree in automation from Northwestern Polytechnical University, Xi'an, China, in 2014. He is currently an M.S. student with the School of Electrical Engineering, Chongqing University, Chongqing. His current research interests include multiagent systems and optimization of microgrids.

Minglin Wang received the B.S. degree in electrical engineering from Shandong University of Technology, Shangdong, China, in 2012; and the M.S. degree in electrical engineering from Chongqing University, Chongqing, China, in 2015. He is currently an engineer at Weifang power supply company.

Minyou Chen (M'05−SM'14) received the M.Sc. degree in control theory and engineering from Chongqing University, Chongqing, China, in 1987, and the Ph.D. degree in control engineering from the University of Sheffield, Sheffield, U.K., in 1998. He is currently a Full Professor with Chongqing University. His current research interests include intelligent modeling and control, multiobjective optimization, micro-grid control, and state monitoring in power distribution systems.

Josep M. Guerrero (S'01−M'04−SM'08−F'15) received the B.S. degree in telecommunications engineering, the M.S. degree in electronics engineering, and the Ph.D. degree in power electronics from the Technical University of Catalonia, Barcelona, in 1997, 2000 and 2003, respectively. Since 2011, he has been a Full Professor with the Department of Energy Technology, Aalborg University, Denmark. His research interests are oriented to different microgrid aspects, including power electronics, hierarchical and cooperative control, energy management systems, and optimization of microgrids and islanded minigrids. Prof. Guerrero is an Associate Editor for the IEEE TRANSACTIONS ON POWER ELECTRONICS, the IEEE TRANSACTIONS ON INDUSTRIAL ELECTRONICS, and the IEEE INDUSTRIAL ELECTRONICS MAGAZINE, and an Editor for the IEEE TRANSACTIONS ON SMART GRID. He was the chair of the Renewable Energy Systems Technical Committee of the IEEE Industrial Electronics Society.

Derek Abbott (M'85−SM'99−F'05) was born in South Kensington, London, U.K., in 1960. He received the B.Sc. (honors) degree in physics from Loughborough University, Leicestershire, U.K., in 1982 and the Ph.D. degree in electrical and electronic engineering from The University of Adelaide, Adelaide, S.A., Australia, in 1995, under K. Eshraghian and B. R. Davis. Since 1987, he has been with The University of Adelaide, where he is presently a full Professor with the School of Electrical and Electronic Engineering. His interest is in the area of multidisciplinary physics and electronic engineering applied to complex systems. His research programs span a number of areas including networks, game theory, energy policy, stochastics, and biophotonics. Prof. Abbott is a Fellow of the Institute of Physics (IOP) and Fellow of the Institute of Electrical & Electronic Engineers. Prof. Abbott has served as an Editor and/or Guest Editor for a number of journals including the IEEE JOURNAL OF SOLID-STATE CIRCUITS, PROCEEDINGS OF THE IEEE, the IEEE PHOTONICS JOURNAL, *PLOSONE,* and is currently on the editorial boards of Nature's *Scientific Reports*, IEEE ACCESS, *Royal Society Open Science* (RSOS), and *Frontiers in Physics.*